

Effects of substitution of group-V atoms for carbon or silicon atoms on optical properties of silicon carbide nanotubes

Ying-Ying Yang(杨莹莹), Pei Gong(龚裴), Wan-Duo Ma(马婉铎), Rui Hao(郝锐), and Xiao-Yong Fang(房晓勇)
Citation: Chin. Phys. B, 2021, 30 (**6**): 067803. DOI: 10.1088/1674-1056/abdb1e
Journal homepage: http://cpb.iphy.ac.cn; http://iopscience.iop.org/cpb

What follows is a list of articles you may be interested in

Low-dimensional phases engineering for improving the emission efficiency and stability of quasi-2D perovskite films

Yue Wang(王月), Zhuang-Zhuang Ma(马壮壮), Ying Li(李营), Fei Zhang(张飞), Xu Chen(陈旭), and Zhi-Feng Shi(史志锋)
Chin. Phys. B, 2021, 30 (**6**): 067802. DOI: 10.1088/1674-1056/abe92b

Optical polarization characteristics for AlGaN-based light-emitting diodes with AlGaN multilayer structure as well layer

Lu Xue(薛露), Yi Li(李毅), Mei Ge(葛梅), Mei-Yu Wang(王美玉), and You-Hua Zhu(朱友华)
Chin. Phys. B, 2021, 30 (**4**): 047802. DOI: 10.1088/1674-1056/abcf3f

Plasmonic properties of graphene on uniaxially anisotropic substrates

Shengchuan Wang(汪圣川), Bin You(游斌), Rui Zhang(张锐), Kui Han(韩奎), Xiaopeng Shen(沈晓鹏, and Weihua Wang(王伟华)
Chin. Phys. B, 2021, 30 (**3**): 037801. DOI: 10.1088/1674-1056/abd168

Modulation of the second-harmonic generation in MoS_2 by graphene covering

Chunchun Wu(吴春春), Nianze Shang(尚念泽), Zixun Zhao(赵子荀), Zhihong Zhang(张智宏), Jing Liang(梁晶), Chang Liu(刘畅), Yonggang Zuo(左勇刚), Mingchao Ding(丁铭超), Jinhuan Wang(王金焕), Hao Hong(洪浩), Jie Xiong(熊杰), and Kaihui Liu(刘开辉)
Chin. Phys. B, 2021, 30 (**2**): 027803. DOI: 10.1088/1674-1056/abd77f

Optical properties of several ternary nanostructures

Xiao-Long Tang(唐小龙), Xin-Lu Cheng(程新路), Hua-Liang Cao(曹华亮), and Hua-Dong Zeng(曾华东)
Chin. Phys. B, 2021, 30 (**1**): 017803. DOI: 10.1088/1674-1056/abaee6

Effects of substitution of group-V atoms for carbon or silicon atoms on optical properties of silicon carbide nanotubes*

Ying-Ying Yang(杨莹莹), Pei Gong(龚裴), Wan-Duo Ma(马婉铎), Rui Hao(郝锐), and Xiao-Yong Fang(房晓勇)†

Key Laboratory for Microstructural Material Physics of Hebei Province, School of Science, Yanshan University, Qinhuangdao 066004, *China*

(Received 8 October 2020; revised manuscript received 18 December 2020; accepted manuscript online 13 January 2021)

Silicon carbide nanotubes (SiCNTs) have broad application prospects in the field of micro-nanodevices due to their excellent physical properties. Based on first-principles, the difference between optical properties of SiCNTs where C atom or Si atom is replaced by group-V element is studied. The results show that the optical absorptions of SiCNTs doped by different elements are significantly different in the band of 600 nm–1500 nm. The differences in photoconductivity, caused by different doping elements, are reflected mainly in the band above 620 nm, the difference in dielectric function and refractive index of SiCNTs are reflected mainly in the band above 500 nm. Further analysis shows that SiCNTs doped with different elements change their band structures, resulting in the differences among their optical properties. The calculation of formation energy shows that SiCNTs are more stable when group-V element replaces Si atom, except N atom. These research results will be beneficial to the applications of SiC nanomaterials in optoelectronic devices and provide a theoretical basis for selecting the SiCNTs' dopants.

Keywords: silicon carbide nanotubes, group-V doped, optical properties, first-principles theory

PACS: 78.67.Ch, 78.20.Ci, 71.55.–i, 71.15.Mb **DOI:** 10.1088/1674-1056/abdb1e

1. Introduction

The silicon carbide (SiC) nanomaterials have excellent mechanical, thermal, electrical, and optical properties,[1–4] and they have been widely used in electronic devices, optical devices, and other fields.[5–7] Therefore, they have attracted much attention of many scholars.[8–12] SiCNT is an important low-dimensional material, which not only has the excellent characteristics of SiC crystal, but also shows some unique characteristics of nanotubes.[13–17] The unique optical characteristics of semiconductor SiCNT provide the possibility for its applications in optoelectronic devices.[18–20] Therefore, since SiCNT was synthesized experimentally,[21,22] it has been widely used as a nano-optoelectronic device material with broad application prospects, and has been widely concerned by the researchers.[23,24]

As an important method to adjust material properties, the dopant effects on electronic and optical properties of semiconductors have been studied.[25–28] For SiCNTs, group-V elements are the donor dopants, so studying the optical properties of group-V elements-doped SiCNTs is of great significance in the applications of SiC nano-optoelectronic devices. In recent years, there have been many reports on the influence of dopants on the properties of SiCNTs. For example, In 2009, Bao *et al.* studied the effects of N-doping on the optical properties of zigzag SiCNTs. The studies showed that N-doping reduces the value of absorption peak and produces many new absorption peaks.[29] In 2014, Behzad *et al.* studied the effects of Ga-doping on the optical properties of zigzag SiCNTs. The optical studies based on dielectric function indicated that new transition peaks and a blue shift are observed after Ga-doping.[30] Khodadad *et al.* investigated the structural and electronic properties of Li-doped SiCNTs. The calculations demonstrated that the doping of Li atom changes some physical properties of pure bundled NT. Owing to charges transferring from Li to SiCNTs, the most significant effect of Li intercalation on the electronic band structure is the shift of Fermi energy.[31] In 2018, Gong *et al.* studied the effect of group-III doping on the optical properties of SiCNTs. The study results showed that group-III element doping increases the minimum dielectric constant value, thereby increasing the transmittance; at the same time, it also introduces weaker absorption and dispersion in the near-mid-infrared region, and as the diameter of the doped atoms increases, the response peak is blue shifted.[32] In 2001, Huu *et al.* used the shape memory synthesis method, and achieved the first reproducible synthesis of SiCNTs of different internal and external diameters.[33] In 2002, one-dimensional silicon carbon nanotubes and nanowires of various shapes and structures were synthesized via the reaction of silicon (produced by disproportionation reaction of SiO) with multiwalled carbon nanotubes (as templates) at different temperatures.[21] In 2013, Romain

*Project supported by the National Natural Science Foundation of China (Grant Nos. 11574261 and 51132002) and the Natural Science Foundation of Hebei Province, China (Grant No. A2015203261).

†Corresponding author. E-mail: fang@ysu.edu.cn

© 2021 Chinese Physical Society and IOP Publishing Ltd

et al. fabricated SiCNTs by carburization in silicon nanowires. It was found that the TO peak and LO peak of SiCNTs are at 796 cm^{-1} and 972 cm^{-1} respectively, and the peak of LO is higher than that of TO peak, indicating that the sp^2 and sp^3 bonding configurations exist in SiCNTs.[22]

So far, most of the researches on the SiCNTs doped by group-III elements and group-V elements have focused on structural stabilities, electrical, magnetic or optical aspects. However, most of these studies focus mainly on monatomic doping, and there are few reports on systematically studying the effect of a group of doping elements on the optical properties of SiCNTs. In this paper, the optical properties of SiCNTs doped by group-V elements (N, P, As, and Sb) are systematically studied by using the first-principles, and the optical differences and their effects caused by different substitutions are elaborated theoretically. These studies are of important significance in developing SiCNT nanodevices and putting them into practical applications.

2. Methods and models

Optimization of SiCNTs using CASTEP code was based on first-principles of density functional theory, and the optimization parameters were selected to be the same as those in Ref. [34]. The exchange correlation effect of the interaction between electrons were described by the Perdew–Burke–Ernzerhof (PBE) functional under the generalized gradient approximation (GGA), the plane wave cut-off energy was set to be 330 eV.[35] All the geometries were optimized by using the ultrasoft pseudopotentials until the force on each atom was less than 0.03 eV/Å. All atomic geometry optimizations were performed in the first Brillouin zone, k grid points were $1 \times 1 \times 6$.

The supercell was constructed with twice the minimum unit of the armchair-type (6,6) SiCNTs. In order to reduce the influence of other SiCNTs, a vacuum layer thicker than 10 Å was added outside the supercell, and the optimized model is shown in Fig. 1(a).

Based on this model, the C atoms (marked as N_C-, P_C-, As_C-, and Sb_C-SiCNTs) and Si atoms (marked as N_{Si}-, P_{Si}-, As_{Si}-, and Sb_{Si}-SiCNTs) at the same site of SiCNTs were replaced with group-V elements (N, P, As, Sb). Their optimized models are shown in Figs. 1(b) and 1(c).

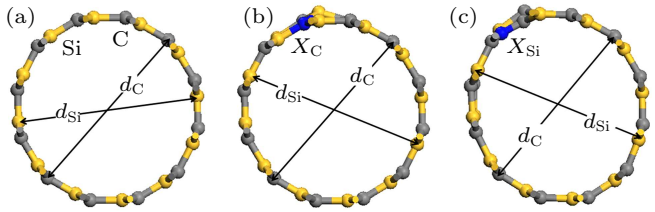


Fig. 1. SiCNTs and their doped SiCNTs structure models, showing (a) undoped SiCNTs, and [(b), (c)] SiCNTs where C atoms and Si atoms are replaced with group-V elements, with X representing group-V elements (X = N, P, As, and Sb), d_C denoting diameter between the C atoms, and d_{Sia} referring to diameter between the Si atoms all in unit of Å.

3. Results and discussion

3.1. Structural stability

The optimized results are shown in Tables 1 and 2, where d_{Si} and d_C are the diameters of Si tube and C tube respectively, and the difference between their values is denoted by $\Delta d = d_C - d_{Si}$ as shown in Fig. 1. It can be seen that in the optimized SiCNTs, Si atoms are on the inside and C atoms are on the outside, and the tube wall thickness of SiCNT is not equal to zero (The wall thickness is about 0.1 Å). Obviously, unlike CNTs, in addition to sp^2 bonding configuration, SiCNT also has an sp^3 bonding configuration. In this paper, although the SiCNT model is sp^2 bonding configuration during modeling, there are both sp^2 bonding configuration and sp^3 bonding configuration after optimization, which is consistent with the experimental results.[22]

Table 1. Optimized structural parameters of SiCNTs with group-V atoms substituting for C atoms.

Structure	Impurity concentration N_d (10^{26}/cm^3)	Chemical potential μ_X (eV/atom)	d_{Si} (Å)	d_C (Å)	Δd (Å)	Total energy E_T (eV)	Formation energy E_F (eV/atom)	Binding energy E_B (eV/atom)
N_C-SiCNT	1.9778	–261.71	10.205	10.301	0.152	6399.39	–0.008	–7.227
P_C-SiCNT	1.9778	–174.33	10.176	10.231	0.126	6306.63	0.104	–7.115
As_C-SiCNT	1.6377	–167.48	9.042	9.301	0.426	6298.97	0.121	–7.098
Sb_C–SiCNT	1.9739	–147.31	10.037	10.115	0.193	–6277.36	0.151	–7.068

Table 2. Optimized structural parameters of SiCNTs with group-V atoms substituting for Si atoms.

Structure	Impurity concentration N_d (10^{26}/cm^3)	Chemical potential μ_X (eV/atom)	d_{Si} (Å)	d_C (Å)	Δd (Å)	Total energy E_T (eV)	Formation energy E_F (eV/atom)	Binding energy E_B (eV/atom)
N_{Si}-SiCNT	1.9814	–261.71	10.142	10.442	0.153	–6443.39	–0.001	–7.216
P_{Si}-SiCNT	1.9955	–174.33	10.184	10.313	0.153	–6354.35	0.034	–7.185
As_{Si}-SiCNT	1.9774	–167.48	10.371	10.527	0.162	–6345.89	0.067	–7.152
Sb_{Si}-SiCNT	1.9456	–147.31	9.575	9.862	0.186	–6324.09	0.101	–7.118

The stability of doped SiCNT structure can be evaluated by the binding energy (or cohesive energy),[36] which is expressed as

$$E_{\mathrm{B}} = \frac{E_{\mathrm{T}} - N_{\mathrm{Si}}\mu_{\mathrm{Si}} - N_{\mathrm{C}}\mu_{\mathrm{C}} - N_X\mu_X}{N_{\mathrm{Si}} + N_{\mathrm{C}} + N_X}, \quad (1)$$

where E_{T} represents the total energy of doped SiCNT, N_{Si}, N_{C}, N_X denote the atom numbers of Si, C, and dopant (N, P, As, and Sb), and μ_{Si}, μ_{C}, μ_X refer to the chemical potentials of Si, C, and doping atoms, where the values of μ_{Si} and μ_{C} are -101.52 (Si), -145.84 (C), respectively. When C (or Si) in SiCNT is replaced, the formation energy can be expressed as

$$E_{\mathrm{F}} = \frac{E_{\mathrm{T}} - E_{\mathrm{T}}^{\mathrm{pure}} - N_X\mu_X + N_X\mu_{\mathrm{C}}\ (\mathrm{or}\ N_X\mu_{\mathrm{Si}})}{N_{\mathrm{Si}} + N_{\mathrm{C}} + N_X}, \quad (2)$$

where $E_{\mathrm{T}}^{\mathrm{pure}} = -6283.15$ eV represents the total energy of pure SiCNT. As shown in Tables 1 and 2, the value of the formation energy of N-SiCNT is negative, indicating that the SiCNT releases the energy in the doping process, the higher the release energy, the more stable the structure is and the easier the doping is to achieve. Therefore, it is easier for N to replace C than Si. The formation energy values of the other dopants are positive, which indicates that the SiCNT absorbs the energy in the doping process. The smaller the absorbed energy, the more stable the structure is and the easier the doping. Comparing the values of the formation energy values among different atoms, it can be found that the stability of SiCNT increases with the doping atom diameter increasing, and the doping becomes more difficult. The substitution for Si atom is easier to achieve than the substitution for C atom.[37] By $\Delta E = E_{\mathrm{B}}(X_{\mathrm{Si}}) - E_{\mathrm{B}}(X_{\mathrm{C}})$ (where X represents group-V atoms (N, P, As, and Sb));[38] except for N doping, when P, As, and Sb replace Si atom, the absolute value of the binding energy is greater than that when replaced with C atom. Therefore, after group-V replaces Si atom, the doped SiCNTs are more stable.

3.2. Optical absorption and photo-induced carriers

Figures 2(a) and 2(b) show the absorption spectra of SiCNTs in the band range of 60 nm–1500 nm after group-V atoms have replaced C and Si atoms, respectively. showing obviously that the differences among effects on optical absorption of SiCNTs in the band range of 60 nm–600 nm by doping different elements are almost negligible. In the frequency band between 600 nm and 1500 nm, there are obvious differences among the optical absorptions of the SiCNTs doped by different elements. From Figs. 2(c) and 2(d), the absorption coefficient of N_C-, P_C-, As_C-, and Sb_C-SiCNT increase slowly, on the contrary, the absorption coefficient of N_{Si}-, P_{Si}-, As_{Si}-, and Sb_{Si}-SiCNT decrease. Especially for N- and P-doped SiCNTs, the absorption coefficient of N_{Si}-SiCNT is about 5000 cm^{-1}, larger than that of N_C-SiCNT.

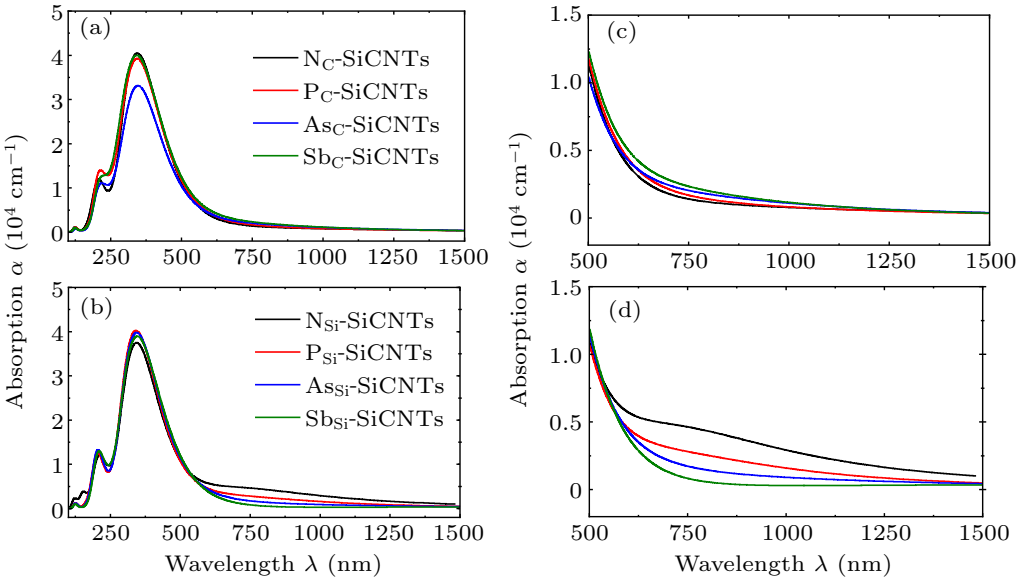


Fig. 2. Optical absorption spectra of SiCNTs where (a) C atom and (b) Si atom are replaced with group-V elements, and [(c), (d)] part of them in a range of 500 nm–1500 nm are magnified.

According to the Tauc equation, the optical absorption α of SiCNT and its energy band structure satisfy the following relationship:[39]

$$(\alpha h\nu)^{1/r} = A\left(h\nu - E_{\mathrm{g}}\right), \quad (3)$$

where A is a constant and $h\nu$ is the photon energy. For a direct band gap semiconductor, $r = 0.5$; for indirect band gap, $r = 2$. Since group-V element-doped SiCNT is still of indirect band gap, $r = 2$. The impurity concentration of doped SiCNT is denoted by N_{d}, and the values for different SiCNTs are shown in Tables 1 and 2. The volume of SiCNT changes little for different doping elements and their displacements, so the impurity concentration does not change much, of them, the impurity concentration of As_C-SiCNTs is the lowest. Figure 2(a) shows that As_C-SiCNT has a minimum absorption peak, which is

caused by the lowest impurity concentration of As_C-SiCNT. According to Fig. 2 and Eq. (3), Tauc fitting was performed for the doped SiCNT photoelectron energy level transition, the process and results are shown in Fig. 3 and Table 3.

Figure 4 shows the band structure of doped SiCNTs, calculated based on the first-principles, where E_c is the conduction band bottom, E_{V1} and E_{V2} are the top and bottom of the upper valence band, respectively, E_{V3} is the top of the lower valence band, and E_{D1}, E_{D2}, and E_{D3} are the impurity levels. Their data are shown in Table 3.

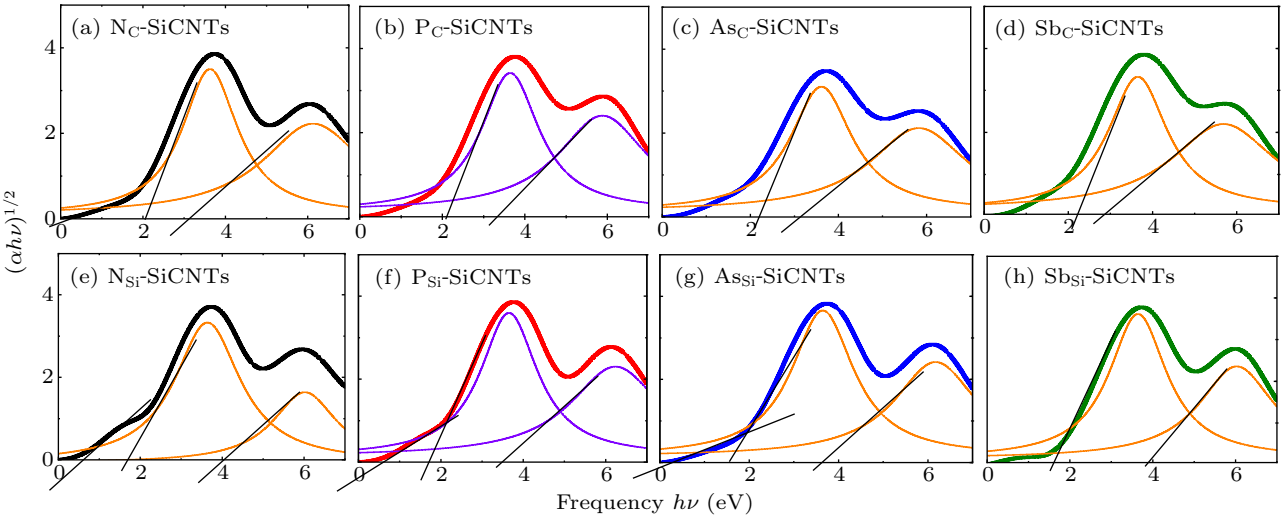


Fig. 3. Tauc fitting of doped SiCNTs, with [(a), (b), (c), and (d)] N, P, As, and Sb substituting for C atoms, and [(e), (f), (g), and (h)] N, P, As and Sb substituting for Si atoms.

Table 3. Electronic (characteristic) parameters of the doped SiCNTs.

	Energy levels (eV)							Ground-excited level jump ΔE (eV)		
	E_C	E_{D1}	E_{D2}	E_{V1}	E_{V2}	E_{D3}	E_{V3}	Region A	Region B	Region C
N_C-SiCNT	0.49	–	0.14	–1.65	–9.89	–	–11.9	0.12	2.20	3.06
P_C-SiCNT	1.05	0.81	0.12	–1.40	–9.26	–	–11.6	0.13	2.16	3.28
As_C-SiCNT	1.20	1.06	0.17	–1.07	–8.98	–	–11.2	0.39	2.25	3.10
Sb_C-SiCNT	1.14	1.02	0.10	–1.18	–9.04	–10.8	–11.4	0.61	2.29	2.84
N_{Si}-SiCNT	0.81	–	0.10	–1.25	–9.34	–10.6	–11.5	0.59	1.70	4.02
P_{Si}-SiCNT	1.02	–	0.16	–1.25	–9.20	–9.99	–11.5	0.60	1.72	3.55
As_{Si}-SiCNT	1.51	–	0.16	–0.74	–8.67	–9.52	–11.0	0.15	1.61	3.63
Sb_{Si}-SiCNT	2.00	–	0.12	–0.20	–8.13	–8.40	–10.4	0.25	1.63	3.86

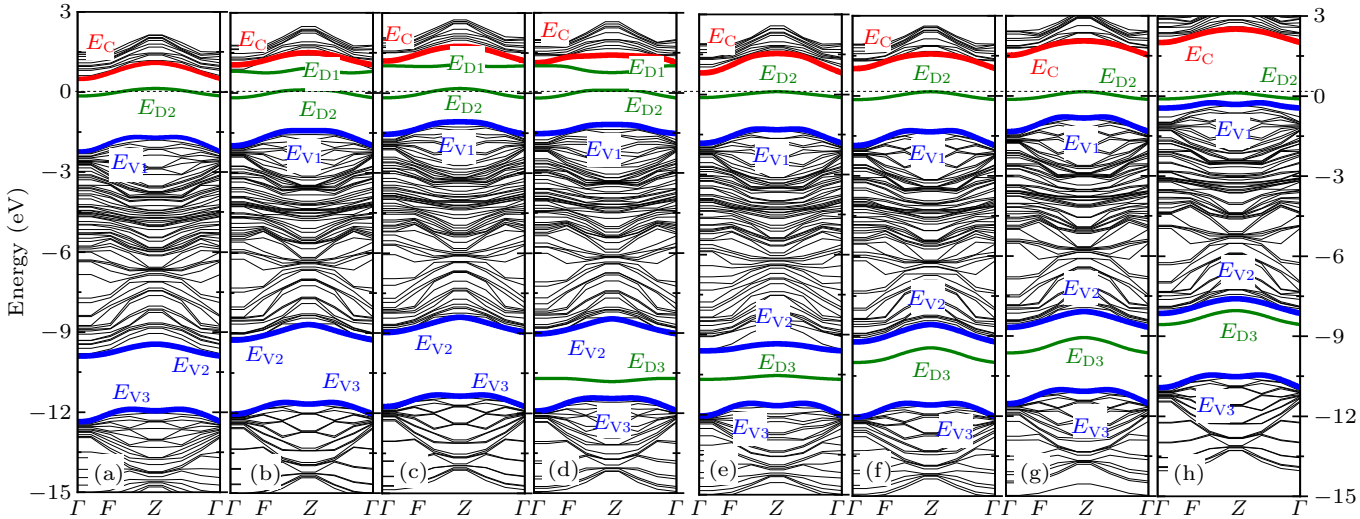


Fig. 4. Energy band structure of SiCNTs with C atoms replaced by (a) N, (b) P, (c) As, and (d) Sb, and Si atoms replaced by (e) N, (f) P, (g) As, and (h) Sb substituting for Si atoms, respectively, and the Fermi level $E_F = 0$.

As can be seen from Fig. 4 and Table 3, when group-V element replaces a C atom, two impurity levels appear in the band-gap of SiCNT: the impurity near the bottom of the conduction band has smaller ionization energy, which belongs to the donor level, and the impurity is easy to form ionized donors; the other impurity level is near the Fermi level, because the ionization energy is larger, the number of electrons provided for the conduction band are much smaller than for the donor level. Most of the unionized impurities are in deep impurity level, and they can be regarded as a recombination center (or trap). When group-V element replaces a Si atom, only one impurity level appears near the Fermi level, the ionization energy is large, and it can also be regarded as a recombination center.

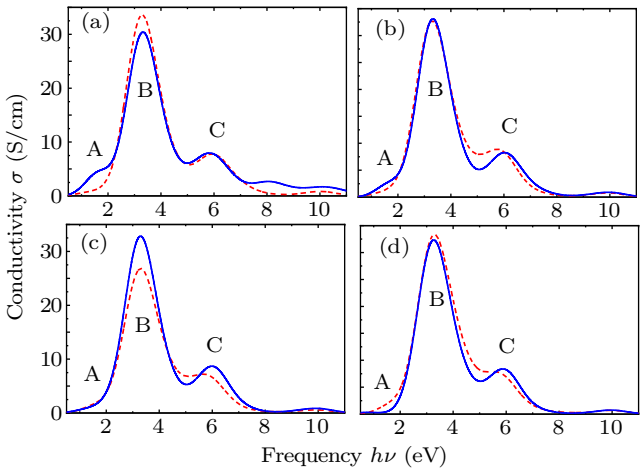


Fig. 5. Photoconductivity spectra of (a) N-, (b) P-, (c) As-, and (d) Sb-SiCNTs, respectively, with dotted line representing substitution of group-V element for C atom, and solid line denoting substitution of group-V element for Si atom.

Figure 5 shows the photoelectric spectra of SiCNTs after C and Si atoms have been replaced by group-V elements, which are mainly composed of three spectral regions A, B, and C. Among them, in the frequency band between 248 nm and 620 nm (B region), doped SiCNTs show a greater photoconductivity. This is because the valence band electrons absorb photons with energy greater than E_g (frequency $v > E_g/h$) and then transfer to the conduction band, thereby generating photo-generated electrons and holes (non-equilibrium carriers). For group-V element-doped SiCNT, the lifetime of photo-generated carriers is on the order of ns, which is much longer than the photon period (corresponding to a frequency of about 10^{14} Hz). Therefore, the photoconductivity generated by the intrinsic excitation of doped SiCNT presents a spectrum width corresponding to a frequency of about 2×10^{14} Hz. In the case where group-V element substitutes for C atom, the conductivity of As_C-SiCNT is the smallest because of its lowest impurity concentration and smallest carrier concentration.[36] Similarly, in the case where group-V element replaces Si atom, because the carrier concentration is the lowest, the conductivity of N_{Si}-SiCNT is also the smallest.

It can be seen from Fig. 4 that the valence band of SiCNT is composed of high part and low part, and the band gap between the two valence bands is about 3 eV.[40] According to the energy band fitting in Fig. 3, it can be judged that the photoconductivity of the 155 nm–248 nm band (C region) is derived from the electronic transition of SiCNTs in the high valence band and the low valence band. When Si atom is replaced, the group-V atom has little effect on the SiCNT valence band. Therefore, the photoconductivity in the C region is almost unchanged; while when C atom is replaced, the p-electron effect of P, As, Sb are enhanced,[36] resulting in a closer relationship between the B spectral band and C spectral band.

The differences among photoconductivities caused by different elements are mainly reflected within the wavelength band above 620 nm (A region), and their spectra are derived from electronic transitions in the conduction band of the impurity level. Among them, the electrons in the shallow impurity level will present the photogenerated carriers in the mid-infrared region of 6.8 μm–16.2 μm. Therefore, the photoconductivity of the A region in Fig. 5 comes from the electrons in the impurity level at the Fermi level. Because the impurity level when C atom is replaced is split into deep part and shallow part, the electron concentration on the impurity level at the Fermi level is less than that in the substitution for Si atom, resulting in a slightly larger conductivity of N_{Si}- and P_{Si}-SiCNTs as shown in Figs. 5(a) and 5(b). In addition, because the ionization energy of Sb atom replacing Si atom is much larger than that of Sb atom replacing C atom, the conductivity of Sb_C-SiCNT is larger than that of Sb_{Si}-SiCNTs as shown in Fig. 5(d).

3.3. Optical refractive index and electron displacement polarization

Figure 6 shows the dielectric spectra of SiCNTs doped with different elements. It can be seen that when the group-V element replaces C atom, the real peak and imaginary peak of the dielectric function of As_C-SiCNTs are the smallest. Within the band less than 600 nm, the dielectric function value of As_C-SiCNT is the smallest, and none of the dielectric functions of N_C-, P_C-, and Sb_C-SiCNTs are significantly different. Within the band above 600 nm, the imaginary part of the dielectric function increases with the doped atomic number increasing, and the real part of the dielectric function increases with the doped atomic number increasing except for the smallest As_C-SiCNT. When group-V element replaces Si atom, the peak value of the dielectric function real part increases with the the number of doped atoms increasing, and the peak shows a significant red-shift phenomenon. The peak value of the N_{Si}-SiCNTs dielectric function imaginary part is the smallest, and the values of other doping conditions are similar. In a frequency band of 500 nm–870 nm, the real part of the dielectric

function gradually increases as the doped atomic number increases, while when it is above 870 nm, the real part of the dielectric function gradually decreases with the atomic number increasing. Within the frequency band greater than 550 nm, the value of the dielectric function imaginary part decreases with atomic number increasing. When group-V element replaces Si atom the dielectric function has more obvious change than when group-V element replaces C atom, and the difference is manifested mainly in a frequency band greater than 500 nm.

Figure 7 shows the refractive index spectra and extinction coefficient spectra of SiCNTs doped with different elements. Comparing Fig. 6 with Fig. 7, it can be seen that the refractive indexes of SiCNTs doped by different substitutions are similar to the real parts of their dielectric constants, and the extinction coefficients are consistent with the imaginary parts of their dielectric constant, satisfying $n \approx \sqrt{\varepsilon'}$ and $\kappa \approx \varepsilon''/2$.

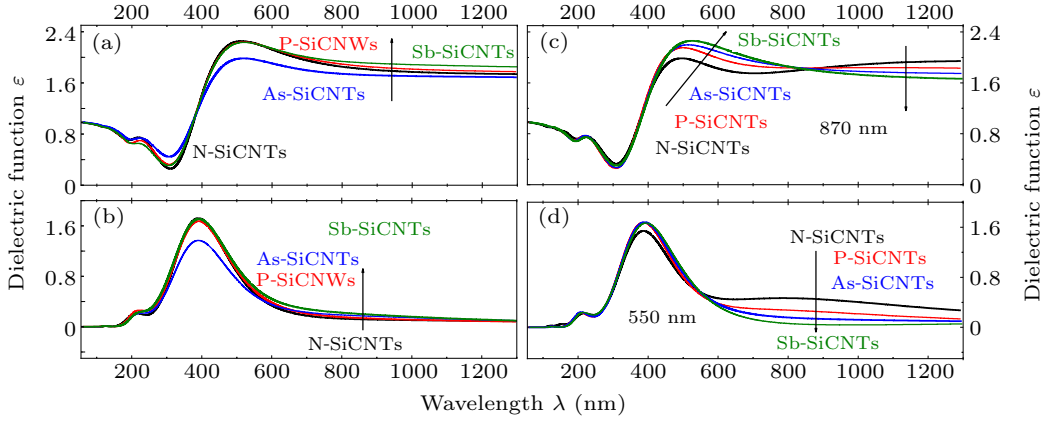


Fig. 6. Dielectric spectra of doped SiCNTs, showing (a) real part and (b) imaginary part for group-V elements replacing C atoms, (c) real part and (d) imaginary part for group-V elements replacing Si atoms.

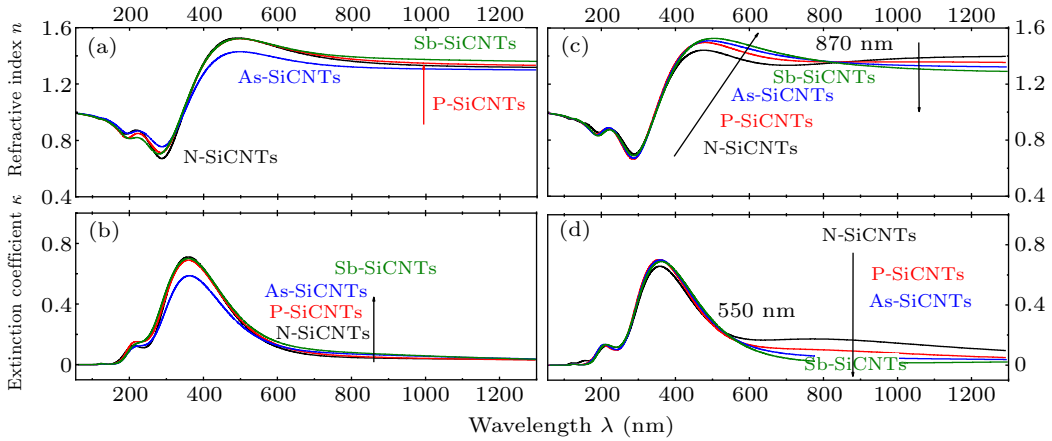


Fig. 7. Refractive properties of doped SiCNTs, showing (a) refractive index and (b) extinction coefficient for group-V replacing C atoms, (c) refractive index and (d) extinction coefficient for group-V replacing Si atoms, respectively.

The dielectric spectrum of semiconductor follows the Lorentz model, and for the doped SiCNT containing multiple spectral peaks can be expressed as[41]

$$\varepsilon(\omega) = 1 + \frac{e^2 N}{m^* \varepsilon_0} \sum_{j=1} \left[\frac{\omega_{j0}^2 - \omega^2}{(\omega_{j0}^2 - \omega^2)^2 + (\omega/\tau)^2} + \mathrm{i} \frac{\omega/\tau}{(\omega_{j0}^2 - \omega^2)^2 + (\omega/\tau)^2} \right], \tag{4}$$

where N and m^* are the electron concentration and the equivalent mass, respectively. The spectrum dielectric behavior of SiCNT is derived from free-electron plasma oscillation, τ denotes the relaxation time, and relates to the damping of the electron plasma oscillation. The oscillation frequency ω_j depends on the electron transitions between different bands. The refractive index of the semiconductor is determined by the electron displacement polarization. According to the electron polarization ratio model, the electron displacement polarization ratio of SiCNT can be expressed as[42]

$$\alpha_e = \frac{2N \left| M_{ij} \right|^2}{E_j - E_i}, \tag{5}$$

where M_{ij} denotes the dipole transition matrix elements between i and j states, and N represents the number of electrons in the transition.

According to the analysis of Fig. 2, Table 3, and Fig. 5, it can be seen that the two spectral peaks near 200 nm and 400 nm are derived from the transition between the valence

band and the conduction band of SiCNT, respectively. Since there are few empty states in the valence band while many empty states in the conduction band, and the energy level difference in the valence band is greater than in the band gap, the dielectric constant and refractive index at 200 nm are much smaller than the values around 400 nm. Similarly, the number of free electrons of doped atoms is much smaller than the valence electrons of SiCNT, resulting in relatively low dielectric constant and low refractive index in the above 500-nm band. In particular, the differences among refractive indexes of SiCNTs, caused by different doping elements are reflected mainly in this frequency band, and their variation law is closely related to the concentration of free electrons in the donor ionization, which is consistent with the dielectric spectrum of Fig. 6. As can be seen from Fig. 7, the refractive index and extinction coefficient of As_C-SiCNT are the lowest because of its lowest impurity concentration.

3.4. Optical dispersion and loss

Dispersion and loss are important parameters to measure the optical properties of material. The dispersion coefficient can be expressed as[32]

$$D(\lambda) = -\frac{\lambda}{c}\frac{\mathrm{d}^2 n(\lambda)}{\mathrm{d}\lambda^2}, \tag{6}$$

where λ is the wavelength, c is the propagation speed of the electromagnetic wave in vacuum, and $n(\lambda)$ is the refractive index of SiCNT. The dispersion spectra of SiCNTs doped by different elements are shown in Fig. 8.

Figure 9 shows the reflectivity and loss factor of SiCNT doped with different elements. The loss factor is also called the loss tangent, which can be expressed as

$$\tan\delta_e = \varepsilon''/\varepsilon', \tag{7}$$

where ε' and ε'' are the real part and imaginary part of the dielectric constant, δ_e is called the electrical loss angle.

It can be seen from Fig. 9 that except for the band near 300 nm, the reflectance of group-V element-doped SiCNT is less than 10% (10 dB), so it does not reflect visible light; N_C-SiCNTs has the largest refractive index when group-V element replaces C atom, followed by As_C-, P_C-, and Sb_C-SiCNTs. When the group-V element replaces Si atom, the refractive index increases with the increase of the number of doping atoms

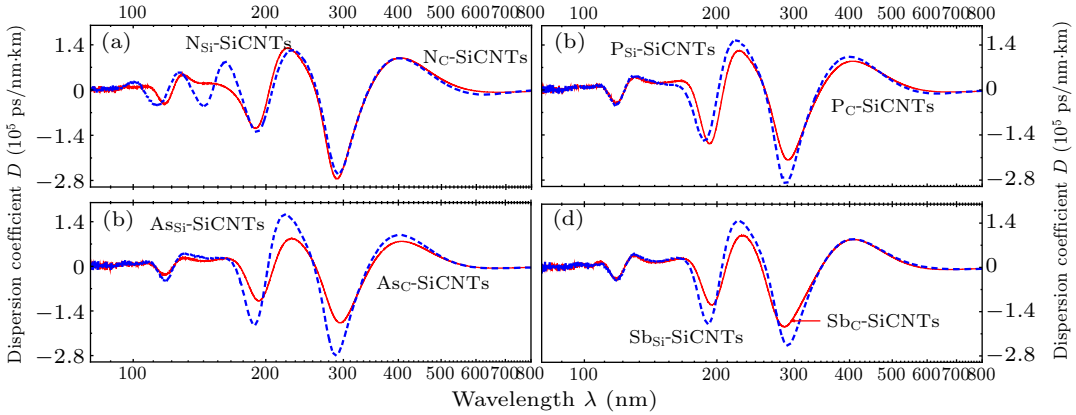


Fig. 8. Dispersion spectra of SiCNTs doped with (a) N, (b) P, (c) As, and (d) Sb respectively. It can be seen from Fig. 8 that when group-V element replaces C atom, the dispersion coefficients of N_C- and P_C-SiCNTs are slightly larger than that of As_C- and Sb_C-SiCNTs, respectively, among them, As_C-SiCNT's impurity concentration is the smallest and dispersion coefficient is the smallest. When group-V element replaces Si atom, there is no significant difference in the dispersion coefficient for doped SiCNT. When group-V element substitutes for Si atom, the dispersion coefficient is larger than that when C atom is replaced, but there is no big difference in the dispersion coefficient when N atom replaces C atom or Si atom.

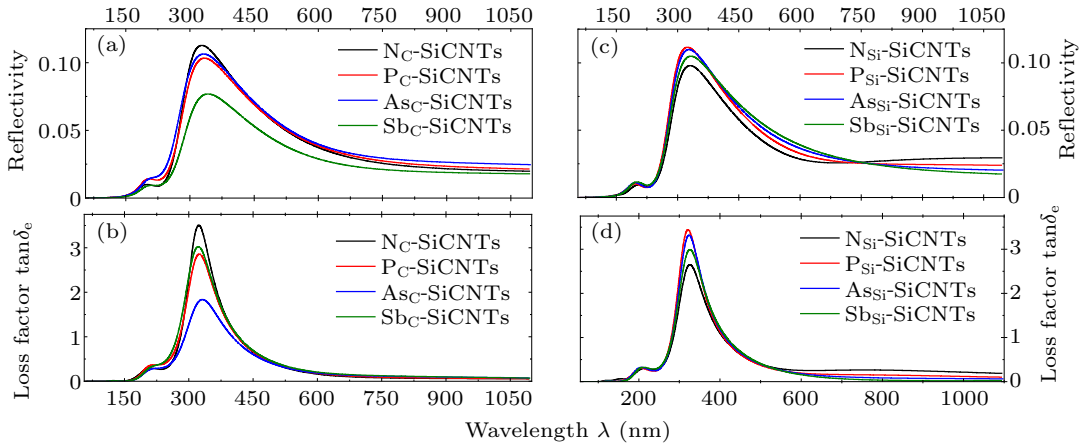


Fig. 9. Reflectance and loss factorfor N, P, As, and Sb replacing [(a), (b)] C atom and [(c), (d)] Si atom.

in the band range of 400 nm–750 nm, and the situation is opposite in the band above 750 nm. Regardless of whether C or Si atom is replaced, the refractive index of SbC-SiCNT is the smallest.

Under optical frequency $\varepsilon'' = \sigma/\omega$, the loss comes mainly from the electronic conductance. When C atom is replaced, the loss of N_C-SiCNT is the largest, and Sb_C-, P_C-, and As_C-SiCNTs decrease in sequence; in the substitution for Si, the loss of N_{Si}-SiCNT is the smallest, and Sb_{Si}-, As_{Si}-, and P_{Si}-SiCNTs increase in sequence, which is similar to the trend of photoconductivity in Fig. 5. Whether C or Si atom is replaced, As_C-SiCNT has the least loss. By comparing Fig. 8 with Fig. 9, it is clear that group-V element-doped SiCNT has a large loss around 300 nm, however, it generates a higher reflection due to the lowest dispersion coefficient in this band.

4. Conclusions

In this work, we have studied the effect on the optical properties of SiCNT where C atom or Si atom is replaced by the group-V element. The results are shown below. In the frequency band between 600 nm and 1500 nm, there are obvious differences among the optical absorptions of different elements doped SiCNTs. Especially for N- and P-SiCNTs, the absorption coefficient of N_{Si}-SiCNT is about 5000 cm^{-1} larger than that of N_C-SiCNT. In the range of 248 nm–620 nm, the doped SiCNT has a greater photoconductivity, and the photoconductivity generated by the intrinsic excitation of doped SiCNT is exhibited within a spectral width corresponding to nearly 2×10^{14} Hz. In the band greater than 620 nm, there are differences in photoconductivity when group-V element replaces C atom or Si atom. When the group-V element replaces Si atom, the dielectric function and refractive index change significantly compared with when C atom is replaced, and the difference is manifested mainly in the frequency band above 500 nm. Regardless of whether C or Si atom is replaced, Sb_C-SiCNT has the smallest refractive index.

References

[1] Ansari R, Mirnezhad M and Rouhi H 2014 *Nano* **09** 1450043
[2] Liu G, Tuttle B R and Dhar S 2015 *Appl. Phys. Rev.* **2** 021307
[3] Toktamiş H and Hama P O 2019 *Applied Radiation and Isotopes* **148** 138
[4] Kityk I V, Makowska J M, Kassiba A and Plucinski K J 2000 *Opt. Mater.* **13** 449
[5] Maboudian R, Carraro C, Senesky D G and Roper C S 2013 *Vac. Sci. Technol. A* **31** 050805
[6] Ivanov P A and Chelnokov V E 1992 *Semicond. Sci. Technol.* **7** 863
[7] Feng X L, Matheny M H, Zorman C A, Mehregany M and Roukes M L 2010 *Nano Lett.* **10** 2891
[8] Attolini G, Rossi F, Negri M, Dhanabalan S C, Bosi M, Boschi F, Lagonegro P, Lupo P and Salviati G 2014 *Mater. Lett.* **124** 169
[9] Pavlikov A V, Latukhina N V, Chepurnov V I and Timoshenko V Y 2017 *Semiconductors* **51** 402
[10] Li Y J, Li S L, Gong P, Li Y L,Fang X Y, Jia Y H and Cao M S 2018 *Physica E* **104** 247
[11] Li Y L, Gong P and Fang X Y 2020 *Chin. Phys. B* **29** 037304
[12] Sha B, Lukianov A N, Dusheiko M G, Lozinskii V B, Klyui A N, Korbutyak D V, Pritchin S E and Klyui N I 2020 *Opt. Mater.* **106** 109959
[13] Zhao J X and Ding Y H 2008 *J. Phys. Chem. C* **112** 2558
[14] Wu A, Song Q, Yang L and Hao Q 2011 *Theor. Comput. Chem.* **977** 92
[15] Zhao M, Xia Y, Zhang R Q and Lee S T 2005 *J. Chem. Phys.* **122** 214707
[16] Zhou X and Tian W Q 2011 *J. Phys. Chem. C* **115** 11493
[17] Gong P, Li Y L, Jia Y H, Li Y J, Li S L, Fang X Y and Cao M S 2018 *Phys. Lett. A* **382** 2484
[18] Huang S P, Wu D S, Hu J M, Zhang H, Xie Z, Hu H and Cheng W D 2007 *Opt. Express* **15** 10947
[19] Behzad S 2015 *Opt. Mater.* **47** 512
[20] Wu I J and Guo G Y 2007 *Phys. Rev. B* **76** 035343
[21] Sun X H, Li C P, Wong W K, Wong N B, Lee C S, Lee S T and Teo B K 2002 *J. Am. Chem. Soc.* **124** 14464
[22] Romain L L, Ollivier M, Thiney V, Pluchery O C and Martin M 2013 *J. Phys. D: Appl. Phys.* **46** 092001
[23] Zhou J Y, Zhou M, Chen Z Y, Zhang Z X, Chen C C, Li R S, Gao X P and Xie E Q 2009 *Surf. Coat. Technol.* **203** 3219
[24] Mercan K and Civalek O 2017 *Composites Part B* **114** 34
[25] Yang K, Li D F, Huang W Q, Xu L, Huang G F and Wen S C 2017 *Appl. Phys. A* **123** 96
[26] Miao H, Huang G F, Liu J H, Zhou B X, Pan A L, Huang W Q and Huang G F 2016 *Appl. Surf. Sci.* **370** 427
[27] Qi K Z, Xing X H, Zada A, Li M Y, Wang Q, Liu S Y, Lin H X and Wang G Z 2020 *Ceram. Int.* **46** 1494
[28] Wang X, Huang S X, Luo H, Deng L W, Wu H, Xu Y C, He J and He L H 2019 *Acta Phys Sin.* **68** 187301 (in Chinese)
[29] Bao S, Zheng J P, Yang G H and Chen J W 2009 *Physica B* **404** 4090
[30] Behzad S, Chegel R, Moradian R and Shahrokhi M 2014 *Superlattices and Microstructures* **73** 185
[31] Khodadad M, Baizaee S M, Yuonesi M and Kahnouji H 2014 *Physica E* **59** 139
[32] Gong P, Li Y L, Jia Y H and Fang X Y 2018 *Chin. Phys. Lett.* **35** 117801
[33] Huu C P, Keller N, Ehret G and Ledoux M J 2001 *Journal of Catalysis* **200** 400
[34] Vanderbilt D 1990 *Phys. Rev. B* **41** 7892
[35] Song J X, Yang Y T, Liu H X and Zhang Z Y 2009 *Acta Phys. Sin.* **58** 4883 (in Chinese)
[36] Yang Y Y, Gong P, Ma W D, Li Y L, Fang X Y, Jia Y H and Cao M S 2020 *Phys. Lett. A* **384** 126602
[37] Gong P, Yang Y Y, Ma W D, Fang X Y, Jing X L, Jia Y H and Cao M S 2021 *Physica E* **128** 114578
[38] Gali A 2006 *Phys. Rev. B* **73** 245415
[39] Wood D and Tauc J 1972 *Phys. Rev. B* **5** 3144
[40] Song J X, Liu H X, Guo Y N and Zhu K R 2015 *Physica E* **74** 198
[41] Jia Y H, Gong P, Li S L, Ma W D, Fang X Y, Yang Y Y and Cao M S 2020 *Phys. Lett. A* **384** 126106
[42] Li Y J, Li Y L, Li S L, Gong P and Fang X Y 2017 *Chin. Phys. B* **26** 047309